



UNIVERSITÀ DEGLI STUDI DI TORINO

This Accepted Author Manuscript (AAM) is copyrighted and published by Elsevier. It is posted here by agreement between Elsevier and the University of Turin. Changes resulting from the publishing process - such as editing, corrections, structural formatting, and other quality control mechanisms - may not be reflected in this version of the text. The definitive version of the text was subsequently published in *Journal of Neuroscience Method*, Volume 187, Issue 1, March 2010, DOI: 10.1016/j.jneumeth.2010.01.001.

You may download, copy and otherwise use the AAM for non-commercial purposes provided that your license is limited by the following restrictions:

- (1) You may use this AAM for non-commercial purposes only under the terms of the CC-BY-NC-ND license.
- (2) The integrity of the work and identification of the author, copyright owner, and publisher must be preserved in any copy.
- (3) You must attribute this AAM in the following format: Creative Commons BY-NC-ND license (<http://creativecommons.org/licenses/by-nc-nd/4.0/deed.en>), <http://dx.doi.org/10.1016/j.jneumeth.2010.01.001>

Calibration of the stereological estimation of the number of myelinated axons in the rat sciatic nerve: A multicenter study

S. Kaplan^{a,1}, S. Geuna^{b,*1}, G. Ronchi^b, M.B. Ulkay^c, C.S. von Bartheld^{d,1}

^a Department of Histology and Embryology, Ondokuz Mayıs University School of Medicine, Samsun, Turkey

^b Department of Clinical and Biological Sciences and Cavalieri Ottolenghi Institute for Neuroscience, University of Turin, Italy

^c Department of Histology and Embryology, Istanbul University School of Veterinary Medicine, Istanbul, Turkey

^d Department of Physiology and Cell Biology, University of Nevada School of Medicine, Reno, NV 89557, USA

Abstract

Several sources of variability can affect stereological estimates. Here we measured the impact of potential sources of variability on numerical stereological estimates of myelinated axons in the adult rat sciatic nerve. Besides biological variation, parameters tested included two variations of stereological methods (unbiased counting frame versus 2D-disector), two sampling schemes (few large versus frequent small sampling boxes), and workstations with varying degrees of sophistication. All estimates were validated against exhaustive counts of the same nerve cross sections to obtain calibrated true numbers of myelinated axons (gold standard). In addition, we quantified errors in particle identification by comparing light microscopic and electron microscopic images of selected consecutive sections. Biological variation was 15.6%. There was no significant difference between the two stereological approaches or workstations used, but sampling schemes with few large samples yielded larger differences ($20.7 \pm 3.7\%$ SEM) of estimates from true values, while frequent small samples showed significantly smaller differences ($12.7 \pm 1.9\%$ SEM). Particle identification was accurate in 94% of cases (range: 89–98%). The most common identification error was due to profiles of Schwann cell nuclei mimicking profiles of small myelinated nerve fibers. We recommend sampling frequent small rather than few large areas, and conclude that workstations with basic stereological equipment are sufficient to obtain accurate estimates. Electron microscopic verification showed that particle misidentification had a surprisingly variable and large impact of up to 11%, corresponding to 2/3 of the biological variation (15.6%). Thus, errors in particle identification require further attention, and we provide a simple nerve fiber recognition test to assist investigators with self-testing and training.

1. Introduction

Peripheral nerves are subject to many different types of injuries and diseases (Dahlin et al., 2009; Siemionow and Brzezicki, 2009). Over the last thirty years, various algorithms were developed to quantify morphological parameters of nerves (Matiasek et al., 2008). One of the most important neuropathological indicators of nerve damage and regeneration is the total number of myelinated axons (Vleggeert-Lankamp, 2007; Geuna and Varejão, 2008; Raimondo et al., 2009). Since it is inefficient to count and measure all fibers of a nerve, researchers usually examine only a small part (sample) of the entire group of nerve fibers (population) (Cassel et al., 1993; Geuna, 2000). Reliable quantitative estimation of the total number of myelinated nerve fibers depends on using an appropriate sampling strategy. When sampling errors occur, bias creeps into the estimates (West, 1999; Geuna, 2000; Benes and Lange, 2001; Guillery, 2002; von Bartheld, 2002; Baryshnikova et al., 2006; Canan et al., 2008a).

Attempts to define the most adequate sampling strategy for particle number estimation in quantitative neuromorphology have raised a lively debate (Guillery and Herrup, 1997; Schmitz, 1998; Gundersen et al., 1999; Geuna, 2000; Benes and Lange, 2001; von Bartheld, 2001, 2002; Schmitz and Hof, 2005). Design-based sampling is usually considered the preferable approach to ensure that morphological variables of biological objects do not influence the probability of each object being sampled (Coggeshall and Lekan, 1996; Gundersen et al., 1999; von Bartheld, 2002; Geuna, 2005; Schmitz and Hof, 2005). However, doubts persist regarding the reliability in the practical application in “real” research

contexts (Hatton and von Bartheld, 1999; Guillery, 2002; Farel, 2002; Gardella et al., 2003; Baryshnikova et al., 2006), prompting the task of calibration.

To test the reliability of stereological investigation of peripheral nerves, in this paper we report the results of a calibration study in which we investigated the influence of five different sources of variability: (1) the biological variability; (2) the stereological method used (unbiased counting frame versus 2D-disector); (3) the sampling scheme adopted (few large probes versus frequent small probes); (4) the investigator and type of stereological workstation where the stereological analysis is carried out (multicenter study);

(5) the proper recognition of myelinated axons at the light micro-scopic level (verified by electron microscopy). Our study quantifies these parameters on rat sciatic nerves in a multicenter study and reveals several novel insights that may aid in an improvement of the accuracy of stereological methodology.

2. Materials and methods

2.1. Animals

For axon number estimates and calibration studies, six young adult male Wistar rats weighing between 225 and 300 g were used. The experimental animal protocol was carried out at Ondokuz Mayıs University School of Medicine. From each animal, the right sciatic nerve was dissected under general anesthesia by single intraperitoneal injection of 150 mg/kg ketamine hydrochloride (Ketalar), and a 1-cm long nerve segment was removed just upstream of the sciatic trifurcation. For the axon recognition calibration study, two young adult female Wistar rats weighing between 225 and 250 g were used. The experimental animal protocol was carried out at San Luigi Gonzaga School of Medicine of the University of Turin. From each animal, the right median nerve was dissected under general anesthesia by single intramuscular injection of 3 mg/kg Tiletamine-Zolazepam (Zoletil), and a 1-cm long nerve segment was removed at midway of the humerus. Prior to recovery, animals were euthanized by decapitation. All experimental protocols were reviewed and approved by the local Ethical Committees in accordance with the European Communities Council Directive of 24 November 1986 (86/609/EEC).

2.2. Tissue processing

2.2.1. Axon number estimation and calibration study

Nerve specimens were fixed by immersion in 2.5% glutaraldehyde in 0.1 M phosphate buffer (pH 7.4) for 4–6 h at 4° C, postfixed in 1% osmium tetroxide for 2 h, dehydrated in an ascending alcohol series and embedded in araldite CY212 + 2-dodecenyl succinic acid anhydride (DDSA) + benzyl dimethylamine and dibutyl phthalate mixture. Series of 20 semi-thin (1 μ m thick) transverse sections were cut using an ultramicrotome (LXB 2188 Ultramicrotome, NOVA, Bromma, Sweden) and stained with 1% toluidine blue (Robinson and Gray, 1996; Di Scipio et al., 2008).

2.2.2. Axon recognition calibration study

Nerve specimens were fixed by immersion in 2.5% glutaraldehyde and 0.5% sucrose in 0.1 M Sorensen phosphate buffer for 6–8 h and post-fixed in 1% osmium tetroxide, dehydrated in an ascending alcohol series and embedded in Glauerts' embedding mixture of resins (Raimondo et al., 2009). Series of semi-thin (1 μ m thick) transverse sections were cut using an Ultracut UCT ultramicrotome (Leica Microsystems, Wetzlar, Germany) and stained with 1% toluidine blue. For transmission electron microscopy, ultra-thin sections were cut using the same ultramicrotome and stained with saturated aqueous solutions of uranyl acetate and lead citrate (Robinson and Gray, 1996).

2.3. True fiber number counts and calculation of biological variation

In the six sciatic nerve specimens, the true number of myelinated axons was obtained by extensive counting of all fibers at high-resolution light microscopy and used as the reference gold standard for calibration of the stereological estimates. One section from each nerve was randomly selected and analyzed using a manual stereological workstation composed of a digital camera (Nikon COOLPIX 5400 Tokyo-Japan), a manual dial indicator controlled specimen stage (Kaplan et al., 2001, 2005), and a light microscope (Nikon Microphot-FX, Tokyo-Japan). The area fraction method was followed (Mayhew, 1988; Larsen, 1998) to assure that all fibers were counted. The area of step size (40 μ m \times 40 μ m) and the microscopic counting frame (1600 μ m²) were set up to be equal so that the distance between microscopic fields was zero. In addition, to avoid that a nerve fiber was counted twice when intersecting two adjacent microscopic fields, the unbiased counting frame method with inclusion and exclusion lines was adopted; any profile of a myelinated nerve fiber touching the exclusion lines was excluded from counting (in this study, the lower and left borders including their extensions were used as exclusion lines, see Fig. 1A), while any profile touching the inclusion lines only (the upper and right borders) and located inside the frame was counted (Kaplan et al., 2001, 2005). From these six determinations, the biological variation (BV) was determined as $BV = SD/mean$, because in this case we calculated the true object number and thus sampling error was null (coefficient of error = 0) and thus $BV =$ coefficient of variation (CV) (Mouton, 2002).

2.4. Stereological estimates of myelinated axon number

Three sets of six sections (one for each sciatic nerve randomly selected from the 20 collected for each series) were prepared and sent to the three international centers participating in this study (SCtr1, SCtr2, SCtr3) for independent estimation of total myelinated axon number. In each center two different stereological counting methods, the unbiased counting frame (Gundersen, 1978; Canan et al., 2008a) versus the 2D-disector (Geuna et al., 2000; Raimondo et al., 2009) were used and, for each method, two different systematic random sampling schemes were tested. The first sampling scheme was based on the use of only few "large" counting frames (5400 μ m²) while the second sampling scheme was based on the use of more frequent "small" counting frames (900 μ m²). Thus, 24 independent myelinated nerve fiber estimates were produced by each of the three centers, because six nerves were examined with four method variations: Large square counting frame (LS), small square counting frame (SS), large circular 2D-disector (LC), and small circular 2D-disector (SC). Fig. 2 illustrates the two sampling schemes. The step size between sampling counting frames was designed in order to assure that the total number of counted axons was similar between the two sampling schemes. About 2.5–4% of the total cross-sectional area was sampled, similar to previous studies (6%, Mayhew, 1988; 1.5–3%, Castro et al., 2008).

2.4.1. Unbiased counting frame

This method, originally described by Gundersen (1978) and subsequently applied to peripheral nerve fiber stereology by Larsen (1998) and Kaplan and co-workers (Acar et al., 2008; Canan et al., 2008a,b), is based on the employment of a square counting frame in which two edges (usually left and bottom) are exclusion (forbidden) lines (solid red lines in Fig. 1A). When an axon touches these lines (including their infinite extension), it is excluded from the counting. The upper and right edges of the frame are called inclusion lines (dashed green lines in Fig. 1A), because an axon that touches these lines is included for counting. When an axon touches

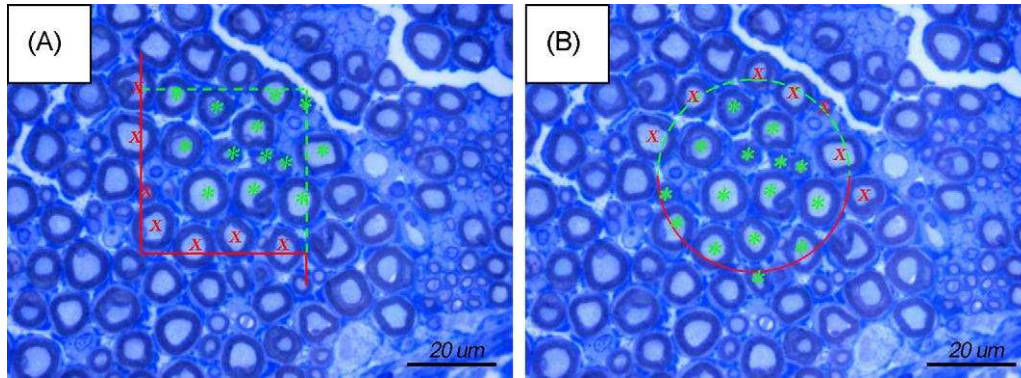


Fig. 1. Sciatic nerve of adult rat, 1 μ m resin cross-sections stained with toluidine blue. (A) Unbiased counting frame method with a square sample area. The nerve profiles marked with a green asterisk in panel A would be included in the counts, but not the profiles marked with a red x. (B) The 2D-disector method with a circular sample area. The nerve profiles marked with a green + in panel B would be included in the counts, but not the profiles marked with a red +. (For interpretation of the references to color in this figure legend, the reader is referred to the web version of the article.)

both an inclusion and an exclusion line, the latter prevails—an axon is thus excluded. In other words, profiles completely or partly within the frame are counted, provided that they do not in any way touch any neighboring frames below or to the left of the current frame demarcated by the exclusion lines and their infinite extensions. For this reason it is necessary to use counting frames that are smaller than the whole monitor/printed area in order to permit the inspection of the “guard area” around each counting frame for verifying that the extensions of a fiber profile that is partly within the frame does not touch any extension of the forbidden lines.

2.4.2. Two-dimensional (2D)-disector

This method is an adaptation of the disector principle used for sampling objects in 3D that is basically an associated-point method, i.e. a method based on the identification of an unambiguous reference point in each particle. It includes the particle in the counting frame only if this point falls inside the frame independently from what happens to the rest of the particle. In the 3D disector method the associated point is usually the “top” of the particle, i.e. the first point that comes into focus while moving from top to bottom along the z-axis (we are referring here to the optical disector, today’s most

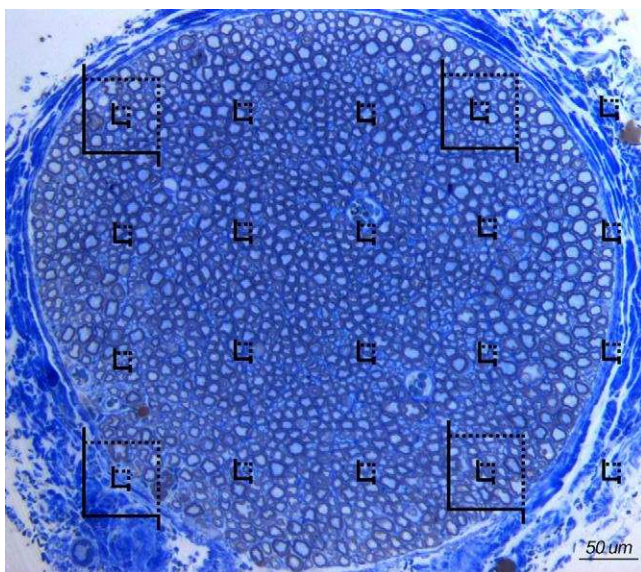


Fig. 2. The systematic random sampling scheme is shown for a cross-section of the sciatic nerve of an adult male rat. The semi-thin, araldite-embedded section was stained with toluidine blue. Sampling schemes with both frequent small sample areas as well as few large sample areas (superimposed) are illustrated.

used stereological method). In the 2D-disector, where the height in the z-axis is not relevant (Gundersen, 1986; Geuna, 2000), the “top” is chosen as the “upper” edge of a fiber profile (Fig. 1B) and thus nerve fibers are considered inside the frame and counted only when their “top” (the point indicated by a cross in Fig. 1B) falls inside the borders of the box.

Unlike earlier descriptions of the 2D-disector (Gundersen, 1986; Geuna, 2000), more recently the adoption of a circular rather than a squared frame has been proposed in order to reduce the probability of nerve fibers (that have a circular shape) to intersect with the frame border (Raimondo et al., 2009). In case a fiber’s top falls exactly on the line and there are thus uncertainties as to whether it is inside or outside the frame, an inclusion hemi circle (the upper dashed green one, Fig. 1A) and an exclusion hemi circle (the lower red solid one, Fig. 1B) are adopted, i.e. when the top of a fiber touches the lower hemi circle it is excluded from counting and vice versa. In very few cases the fiber top falls exactly in the border zone between the inclusion and the exclusion hemi circles, and uncertainties arise about its inclusion for counting: in these cases the rule that “right is in and left is out” is adopted.

2.4.3. Total number estimation from raw stereological data

Starting with the raw data of axon number obtained using the two different stereological protocols, final total number (N) estimation was obtained following two different procedures. SCTR1 and SCTR2 calculated N by multiplying the mean axonal density (D) by the total cross-sectional area (CSA) of the whole nerve measured at low magnification (Geuna et al., 2000). SCTR3 adopted a fractionator approach (Mayhew, 1988; Larsen, 1998; Canan et al., 2008a) which does not require the calculation of the total nerve area and thus avoids the variability arising from differences in the nerve area measurement. In brief, knowing the counting frame size (A_f) and the step size (x-axis, y-axis) between frames (A_{stp}), N was calculated by multiplying the number of fibers counted ($\sum Q^-$) by the sampling fraction area according to the following formula:

$$N = \frac{\sum Q^- \cdot A_{stp}}{A_f}$$

2.5. Specifics of imaging workstations in the study centers

In SCTR1, stereology of nerve fibers was carried out by using an imaging workstation composed of a DM400 microscope, a DFC320 digital camera and an IM50 image analyzer system (Leica Microsystems, Wetzlar, Germany). Fiber counting was carried out on monitor images taken with a 100× immersion oil objective (NA = 1.25). The two types of counting frames were digital images created directly on the monitor. The total cross-sectional area of the nerve was estimated by point-counting with a 20× (dry) objective. The observer was a 34-year old, experienced microscopist.

In SCTR2, stereology of nerve fibers was carried out during direct observation through the microscope, using an Optiphot microscope (Nikon, Tokyo, Japan) with a 100× immersion oil objective (NA = 1.25), and a 10 × 10 square reticule in the eye piece. For the circular sample areas, the circle was projected through a 1.25 drawing tube (Nikon, Tokyo, Japan). The total cross-sectional area of the nerve was estimated by point-counting with a 20× (dry) objective. No software or monitor or digital image acquisition was used. The observer was a 48-year old, experienced microscopist.

In SCTR3, stereology of nerve fibers was carried out using an imaging workstation composed of a Microphot-FX light microscope and a COOLPIX 5400 digital camera (Nikon, Tokyo, Japan). Fiber counting was carried out on monitor images taken with a 100× immersion oil objective (NA = 1.25). The two types of counting frames were printed on transparencies and placed on the monitor. No software for digital image acquisition was used. The observer was a 34-year-old experienced microscopist.

Estimates from the three centers were evaluated for each method by comparing the means of each estimate, as percentage difference from the true value to determine any patterns or statistically significant differences. Percentage difference rather than absolute values were used, because biological variation was

eliminated due to the posthoc knowledge about true values.

2.6. Axon recognition at the electron microscopic level

To verify and calibrate axon recognition, ultra-thin sections cut immediately after a semi-thin section were analyzed using a JEM-1010 transmission electron microscope (JEOL, Tokyo, Japan) equipped with a Mega-View-III digital camera and a Soft-Imaging-System (SIS, Münster, Germany) for the computerized acquisition of the images. In order to obtain pairs of semi-thin and thin sections spaced close enough to allow exact ultrastructural identification of all fiber profiles detectable in light microscopy, the procedure described by Geuna et al. (1998) was applied. A small area was selected on a semi-thin section of the entire nerve profile. The embedding block was then trimmed for ultrathin cutting of the selected area and mounted on the ultramicrotome equipped with a diamond knife. Prior to ultrathin cutting, one final semi-thin “reference” section was cut and then immediately followed by a series of 5 ultra-thin sections. In this way, all fiber profiles identifiable in the thin sections were collected at a distance less than 0.5 μ m from the reference semi-thin section, thus permitting the identification and matching of each nerve fiber profile at both light- and electron microscopic levels.

2.7. The Nerve Fiber Recognition (NFR) test

In order to quantify the degree of fiber recognition, three light microscopic digital images (Supplementary Figs. 1–3) were independently analyzed in the three laboratories. For each of these images, an immediately following series of ultra-thin sections was available. In the three light microscopic images, 535 “objects” were marked by a small open circle. These objects generally resembled myelinated nerve fibers, but also included other tissue structures such as Schwann cell nuclei and blood vessels. Then, each laboratory was asked to code in green color all circles corresponding to objects considered myelinated axons, to code red all circles considered other tissue structures, and finally to code in yellow all those cases in doubt. When all scored pictures were collected, extensive electron microscopy observation was carried out on the corresponding ultra-thin sections and all particles indicated by circles in the light micrographs were identified with certainty as either true myelinated axons ($n = 424$) or other tissue structures ($n = 111$). The percentage of recognition errors made by each laboratory was then calculated. The percentage of recognition errors made by each laboratory was then calculated.

2.8. Statistics

Data collected for this methodological study were analyzed in several ways; for each nerve, the difference between the estimate from each center and the true value was calculated and compiled as a percent difference. These percent differences were compared for the different sampling schemes, and also compared with the biological variation. In addition, the differences of the means (for all nerves) were calculated for the three centers. Furthermore, a reliability analysis between the results of centers was conducted, and the Groups’ means comparison between centers. The Groups’ means were compared by Friedman test and then multiple comparisons between pairs of groups were carried out according to Dunn test. Data are shown as mean \pm SEM. A p-value less than 0.05 was considered statistically significant. Statistical analyses were performed using the SPSS software (Statistical Package for the Social Sciences, Version 13.0, SSPS Inc., Chicago, IL, USA).

3. Results

The typical quality of sections through myelinated axons of the adult rat sciatic nerve is shown in Figs. 1 and 2. The true, gold standard exhaustive counts of myelinated axons at a level just upstream of the trifurcation in the six Wistar rat sciatic nerves ranged from 5685 to 8776 (see Fig. 3). The mean was $7354 \pm$

469 (SEM) nerve fibers, consistent with previous published reports of about 7100–8300 myelinated fibers in this nerve (e.g., Schmalbruch, 1986; Castro et al., 2008). In those two studies, the ranges were 7038–9250 ($n = 18$) and 5210–10,010 ($n = 7$), with means of 7825 ± 622 (SD) and 8060 ± 1500 (SD), respectively. Thus, we confirm considerable variability between animals.

3.1. Biological variation

In general, two types of sources contribute to the total variability of stereological estimates, biological variation (BV) and stereological error, typically expressed as coefficient of error (CE). Usually, biological variation can only be estimated, but in our study BV could be precisely measured, based on the gold standard counts (determinations) in our sample population: $BV = SD/\text{mean}$, and BV was calculated to be 15.62%. Biological variance $(BV)^2$ thus was 0.0244, a value that is considered fairly normal for this type of study (Mouton, 2002). Since $(BV)^2 = (CV)^2 - \text{mean}(CE)^2$ (Mouton, 2002), and CV can be measured, we can calculate $(CE)^2$. Thus, based on the values in Table 1, the statistical error for each stereological method and sampling scheme, as well as for each workstation/center can be calculated as shown in Table 1.

3.2. Comparison of stereological methods

Our study was designed to test two different counting protocols as described in Sections 2.4.1 and 2.4.2. There was no significant difference in the accuracy of estimates between the data obtained by the unbiased counting frame (SS, LS) and the 2D-disector (SC, LC) (compare Fig. 3A with 3C, or Fig. 3B with 3D). While one of the three centers (SCtr3) used a fractionator procedure for calculating the total number of fibers from the number counted in the sampling probes, the other two centers used a traditional method which samples fiber density and then multiplies to account for the total cross-sectional area of the nerve. We have thus determined if differences in estimates may reflect

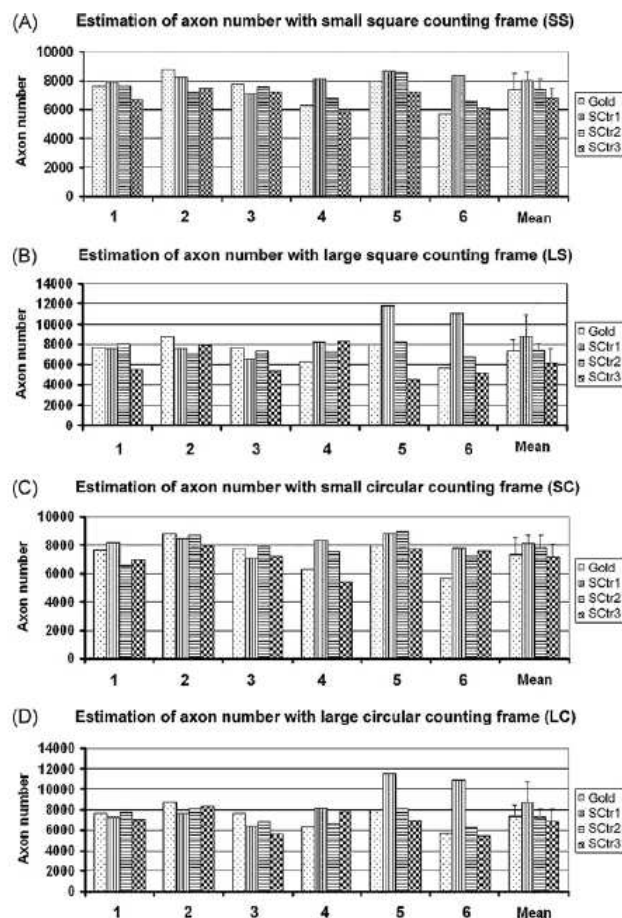


Fig. 3. Estimation of the number of myelinated axons in six sciatic nerves (numbered 1–6 on x-axis) using two different stereological probes (square unbiased counting frame versus circular 2D disector) in combination with two sampling schemes (frequent small samples versus few large samples). (A) Small square unbiased counting frame (SS). (B) Large square unbiased counting frame (LS). (C) Small circular 2D-disector (SC). (D) Large circular 2D-disector (LC). Mean \pm SEM are shown for the means of estimates. The coding of bars indicates study centers (SCTR1, SCTR2, SCTR3) or “gold” (=gold standard exhaustive counts), as listed on the right.

differences in the measurement of the cross-sectional area of the entire nerve profile by comparing measurements between two of the centers. As can be seen in Fig. 4, values in SCTR1 and SCTR2 tended to be nearly identical. This suggests that total nerve area was much less variable between centers than the final estimates. We conclude that variability in the parameter of total nerve area

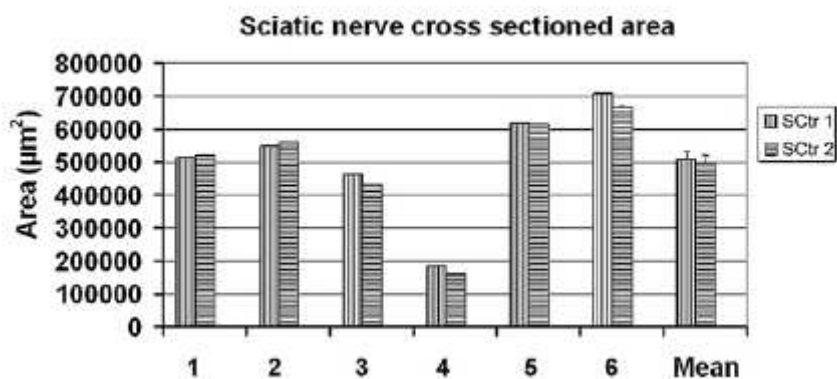


Fig. 4. The group means and estimations of the cross sectional area (CSA) for each sciatic nerve (numbered 1–6) performed by SCTR1 and SCTR2 (mean). The SEM is shown only for the mean estimation. There was no significant difference between the two centers that used the CSA for number estimation. SCTR3 used a different (fractionator) approach and therefore did not calculate the CSA.

was minimal and not relevant for variability in final fiber number estimates.

3.3. Comparison of sampling schemes

Comparing the sampling scheme that uses fewer larger samples (5400 m2) with the scheme that uses more frequent smaller samples (900 m2), there was a statistically significant difference for more, and greater deviations from the gold standard (compare Fig. 3A with B and Fig. 3C with D). As shown in Table 1, the CV and (CV)² (and thus the statistical error) tended to be larger with few large samples (LS and LC) than with frequent small samples (SS and SC), resulting in an unfavorable ratio of statistical and biological error. When all SS and SC estimates were compared with all LS and LC estimates, the former were $12.75 \pm 1.86\%$ (SEM) different from the true values, while the latter differed by $20.71 \pm 3.67\%$ (SEM)—a statistically significant difference (Students t-test, $p < 0.05$). We conclude, consistent with results from computer simulations (Schmitz, 1998), that more frequent but smaller samples are more representative for peripheral nerve axon counting than few large samples.

3.4. Differences between study centers

Our study was designed to evaluate not only different sampling schemes and stereological methods, but also the impact that different types of workstations may have on the accuracy of stereological estimates. Therefore, each study center produced stereological estimates of the number of myelinated axons for each nerve under four different conditions, as compiled in Fig. 3A–D. These estimates were then compared with the gold standard true values for each nerve. This approach allowed us to assess possible bias, accuracy, and other stereological parameters for each study center (Table 1). There are two different ways to measure differences between estimates. One is to only compare overall means, regardless of

Table 1 Sampling errors in stereological estimations using different methods and workstations. Values normalized so that 100% = true value (gold standard) determined by exhaustive counts.

Method	Workstations												
	SCTR1 (Turin)				SCTR2 (Reno)				SCTR3 (Samsun)				
	Mean	CV	(CV) ²	S/B	Mean	CV	(CV) ²	S/B	Mean	CV	(CV) ²	S/B	
SS	112.35	19.2	0.037	60/4	102.02	11.17	0.012	34/66	93.43	8.63	0.007	23/77	
LS	123.92	34.92	0.122	83/1	102.97	13.49	0.018	43/57	85.20	31.24	0.098	80/2	
SC	112.57	16.74	0.028	53/4	107.43	13.84	0.019	44/56	98.57	17.95	0.032	57/43	
LC	122.17	34.46	0.119	83/1	99.85	7.86	0.006	20/8	94.62	18.137	0.033	57/43	

Abbreviations: SS, Small squared samples; LS, large squared samples; SC, small circular samples; LC, large circular samples; CV, coefficient of variation; (CV)², coefficient of variance; SE/BE, ratio of statistical error (S) and biological error (B) (in percentage, with biological variance (BV)² = 0.0244 determined by exhaustive counts of the six nerves); mean of estimates for six nerves = percentage of true value.

Deviation from the true number (gold standard) of axons (mean) for each center and probe

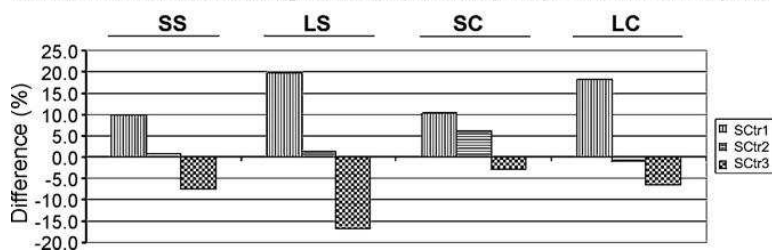


Fig. 5. Differences between the mean estimation from three study centers (SCTR1, SCTR2, SCTR3) of the myelinated axon number using two different stereological probes (square unbiased counting frame versus circular 2D-disector) in combination with two sampling schemes (frequent small versus few large samples). SS, Small square unbiased counting frame; LS, large square unbiased counting frame; SC, small circular 2D-disector; LC, large circular 2D-disector.

biological variability with some nerves containing less than 6000 and others nearly 9000 myelinated axons. The other way is to measure the difference (as a positive number) from each individual true value—regardless whether it is a too large or too small number, and to express this as a percentage of the true value to normalize for biological variation and thus to only evaluate stereological (sampling) variation. This number better reflects the magnitude of deviation, although positive and negative deviations do not cancel out and thus the numbers exaggerate the error. Therefore, it is useful to compare the deviations with the biological variability for a more meaningful assessment of the practical application of the stereological technique, as shown in Fig. 5 and Table 1.

3.4.1. Trends/biases

As seen in Fig. 3 and Table 1, there were some differences between study centers, in that estimates in SCTR1 were generally 12–22% above the true number, in SCTR3 about 1–15% below the true number, and in SCTR2 by 0–7% above the true number. However, none of these differences between centers were statistically significant. Since SCTR2 utilized the least sophisticated workstation, but generated estimates closest to the true values (gold standard), we conclude that sophisticated equipment is not essential for generation of accurate stereological estimates.

3.4.2. Variability/statistical error

As shown in Table 1, the coefficient of variance differed between centers. In SCTR1, the (CV)² was relatively high with 0.028–0.122, while in SCTR2 it was relatively low with 0.006–0.019, and in SCTR3 it varied between 0.007 and 0.098.

3.4.3. Ratio of biological and stereological variance

In 13 of the 16 estimates, the statistical error contributed 60% or less to the total error, consistent with the rule of thumb that statistical or stereological variance should not contribute more than about one half to the total variance (CV)² (Gundersen and Jensen, 1987; Slomianka and West, 2005). It is relevant to note that in all three of the cases with high ratios of stereological error (83%, 83% and 80%, relative to biological variability), the estimates were generated with the sampling scheme of few large samples (Table 1), a sampling scheme that is therefore not recommended as mentioned above.

The mean of all the twelve independent estimates (4 protocols applied in the 3 centers) was remarkably similar to the gold standard mean of 7354, namely the “mean of means” was 7546, which is only 2.6% above the gold standard mean. The groups’ means comparison was statistically evaluated by Friedman test, followed by inter-pair multiple comparisons by Dunn test. This analysis showed that there were no significant differences between the mean axon number estimates obtained in the three centers and the gold standard.

In the course of this multicenter study, we encountered two types of computational mistakes that were made. Despite the experience of all three investigators, there was one instance of incomplete data transfer in SCTR2, resulting in a too low estimate in one of the nerves. This error was recognized (and subsequently corrected) because of the comparative nature of this study—it may have been overlooked in any “normal” study. Likewise, the data in SCTR3 initially were affected by a systematic error that was recognized early in the study and was remedied. We mention this, because most studies do not use back-up, correction or calibration steps to double-check and verify the estimates. This may be a factor that contributes to some of the variability of quantitative data that has been reported in the recent literature (Guillery and Herrup, 1997; Schmitz et al., 1999; von Bartheld, 2001, 2002).

3.5. Recognition of myelinated axons: comparison by light- and electron microscopy

Independently of the stereological protocol used, the proper recognition of myelinated axons at light microscopy is a factor which could potentially influence the final axonal estimates. Therefore, we carried out a calibration study to verify the identification of myelinated axons at light microscopy by examination at the electron microscopic level.

Fig. 6 shows the results of the identification of nerve fibers on consecutive semi-thin and thin sections. Panel A shows a high resolution light microscopic digital image of a semi-thin section (the type of images used for carrying out stereology of fibers); panel B shows electron micrographs of a thin section cut at a distance less than 0.5 μ m from the semi-thin section, focusing on the small light micrograph’s area as indicated in the inset in panel A. Five histological structures are indicated by arrows and numbered: (1) “unmyelinating” Schwann cell nucleus; (2, 4) small myelinated axons; (3) cluster of unmyelinated axons; (5) “myelinating” Schwann cell nucleus with neighboring myelinated axon. Note how the Schwann cell nucleus and the myelinated axon indicated by number 1 and 2, respectively, have exactly the same appearance at light microscopy observation, since the thin myelin sheaths of the small axon are very similar to the dense chromatin ring which borders the glial nucleus. Unmyelinated nerve fibers can only be approximately identified as axon clusters at light microscopy (Fig. 6C). Finally, comparative light and electron microscopic observation reveals how some myelinated axons that are barely visible at light microscopy (Fig. 6A, arrow numbered 4), turn out to have more than twenty myelin lamellae at electron microscopical examination (Fig. 6D and E).

3.6. The Nerve Fiber Recognition test

Results of the quantitative analysis of axon recognition at light and electron microscopic levels between our three centers showed that the percentage of incorrect identifications ranged from 1.2% to 11.1%. In most cases, the mistakes were false positive, i.e. other structures were recognized as axons (range 0.6–10.7%), while only rarely were nerve fibers not recognized as such (range 0.4–0.6%). In 73% of the cases in which other histological structures were incorrectly identified as axons, they actually were Schwann cell nuclei. In addition, the percentage of ambiguous cases, i.e. nerve fibers that raised doubts, ranged from 4.7% to 7.7%. Finally, we also calculated the percentage of recognition errors that were shared between the centers. We found that 57% of mistakes were common to at least two of the centers, suggesting that in the majority of cases, problems arise from the ambiguity of images of histological objects rather than being caused by an individual observer's mistake or oversight.

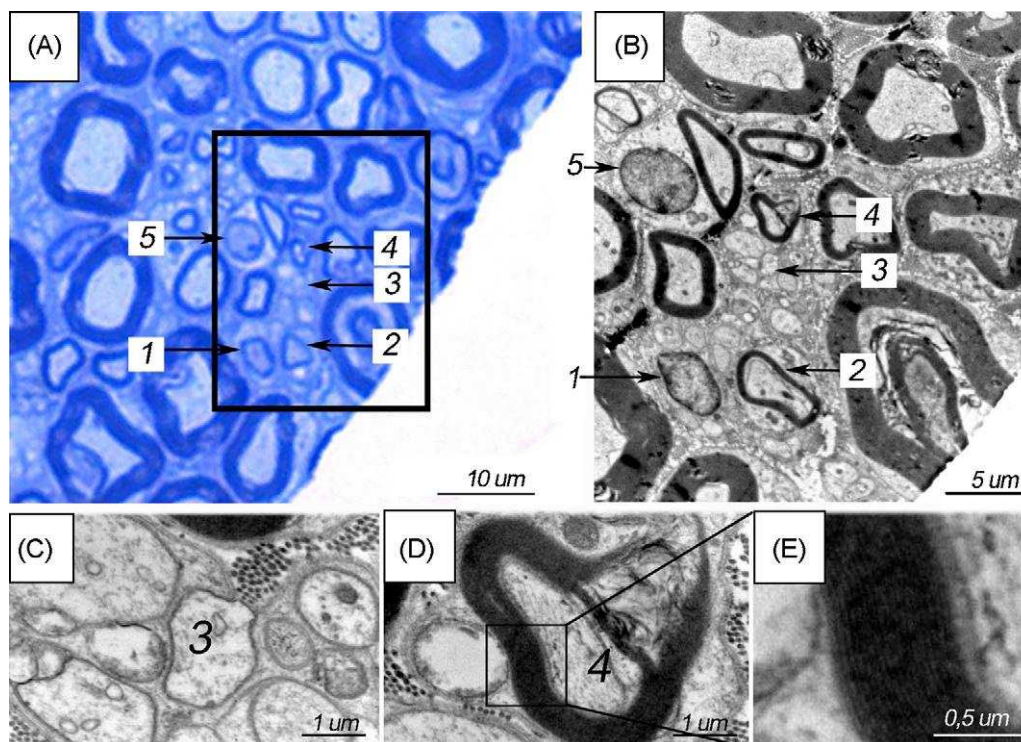


Fig. 6. (A) High resolution light microscopic digital image of a semi-thin section through the sciatic nerve. (B) Electron micrograph of the rectangular area depicted in (A). Arrows point to (1) “unmyelinating” Schwann cell nucleus; (2, 4) small myelinated axons; (3) cluster of unmyelinated axons; (5) “myelinating” Schwann cell nucleus with neighboring myelinated axon. (C) Higher magnification of the unmyelinated fibers. (D and E) Higher magnification of the small myelinated axon numbered 4 (panel D) and its ~20 myelin sheaths (panel E).

The NFR test is available for viewing and for download in the supplementary material. This test may be useful for testing and for training to reduce misidentification of myelinated axon profiles at the light microscopic level.

4. Discussion

Design-based stereology represents an important advance in quantitative morphological assessment of tissues and organs (Sterio, 1984; Gundersen et al., 1988a,b; Hyman et al., 1998; Geuna, 2005; Schmitz and Hof, 2005). The basic concepts of design-based stereology are spreading due to the increasing number of papers adopting stereological methods as well as instructional courses that are being offered worldwide. Therefore, although still slow, the adoption of stereological approaches is expected to further increase. Given that the theoretical “intrinsic strength” of design-based stereological methods is generally accepted among morphologists, what appears to be the main issue of contention is the validity of the

application of stereological principles to quantify actual microscopic images of tissue samples in real study settings. So far, the focus has been mainly directed at comparing design-based and model-based methods (Pover and Coggeshall, 1991; Hatton and von Bartheld, 1999; Basgen et al., 2006; Baquet et al., 2009), at systematic error related to z-axis shrinkage (Guillery, 2002; von Bartheld, 2002, in press; Gardella et al., 2003; Baryshnikova et al., 2006), and the type of embedding medium (Ward et al., 2008), while other potential sources of variability have received less attention. To partially fill this gap, in the present study we assessed five potential sources of variability: 1. biological variability; 2. variations of the stereological method; 3. sampling schemes; 4. workstations; and 5. particle recognition.

First, we measured the biological variance (BV)² and compared it with the stereological variance (CV)². We found that when the “small frequent” sampling scheme was used, the stereological variance was in the same range as biological variability in all three study centers, indicating that the stereological approach to estimate the number of peripheral nerve fibers was adequate. Biological variability was relatively large with 15.6%. This may be due in part to variations in the contributions of different segments and the differing localization of some nerve branches (Schmalbruch, 1986). However, similar variability in myelinated nerve fiber numbers has been reported in previous studies (e.g., Schmalbruch, 1986; Castro et al., 2008).

Second, we measured the potential impact of the stereological method on the variability by comparing the unbiased counting frame and the 2D-disector methods. Results revealed no statistically significant differences between the estimates obtained by means of the two stereological methods. In addition, our results showed that the shape of the frame sample area (squared or circular) does not exert any significant influence on estimation. It can also be concluded that adoption of the fractionator procedure, which requires a sophisticated automated workstation (Canan et al., 2008a,b), is not essential for accurate peripheral nerve fiber stereology, because the center (SCtr3) which adopted the fractionator did not show any significant improvement in accuracy compared with the other workstations (Figs. 3 and 5). In addition, the variability in assessing nerve cross-sectional area (which is not required when a fractionator procedure is adopted) was negligible, supporting the view of Schmitz and Hof (2005) that the variability in the sampling and counting procedure is practically much more relevant for the final total object number estimates than the determination of the total area of the region under investigation.

Third, we compared two types of sampling schemes, few large probes versus frequent small probes. When smaller and more frequent samples were taken, this rendered significantly less variability and difference from true values than fewer, and even larger (overall) samples. Intriguingly, sampling 4–5% of the total cross-sectional area in few large samples (1.5% each) lead to estimates that were less accurate (and therefore less efficient) than those generated by sampling 2–3% of the total area, but in many smaller samples (0.2–0.3% each). Although recommendations on sampling have been made (Gundersen and Osterby, 1981), the optimal number and the size of the probes has been controversial (Popken and Farel, 1996; Geuna et al., 2000; Benes and Lange, 2001; Guillery and August, 2002). Some studies have recommended small but frequent probes (Schmitz, 1998), while others have argued for larger probe sizes (Benes and Lange, 2001; Canan et al., 2008a). Results of the present study validate the recommendations based on computer simulations put forward by Schmitz (1998) that had prompted criticism for the lack of “real world settings” (Benes and Lange, 2001). The superior performance of multiple small disector probes is probably linked to the fact that this sampling scheme provides a better sample representation of the heterogeneous fiber populations within the nerve.

Fourth, we assessed the variability arising from the different laboratory workstations where stereological analysis was carried out. Results revealed trends, but no statistically significant differences between centers. As might be expected, human factors appear to give rise to trends that result in modest fluctuations around the true values. An interesting conclusion that we can draw from the comparison of the stereological estimates from the three different centers is that accurate stereological measurements do not require advanced quantitative microscopy workstations. Although it has been reported that basic

stereological analysis can be performed without sophisticated and expensive stereological equipment (Howard and Reed, 1998; Kaplan et al., 2001; Schmitz and Hof, 2005), it is often assumed that design-based methods require expensive equipment such as video cameras, monitors and computer software (Clarke and Oppenheim, 1995; Guillery and Herrup, 1997). It is therefore of interest to note that among the three workstations tested, the one with the simplest, rudimentary equipment (a microscope with a z-axis encoder and drawing tube, but no video camera, monitor and computer) performed equally or even better (less variance and less extreme deviations, Table 1) than the other two workstations with more sophisticated equipment.

Fifth, we verified to which extent subjectivity in the recognition of myelinated axons at the light microscopic level can influence the final axon estimates. We compared axon recognition by using light and electron microscopy (considering electron microscopy the gold standard for nerve fiber identification, since all fibers can be identified without any doubt). Our quantitative calibration study showed that myelinated nerve fiber identification was 94% accurate on average. The main type of error was related to the thin myelin sheath of small axonal profiles that can be difficult to distinguish from the dense chromatin ring which borders Schwann cell nuclei. On the other hand, although larger axons are usually easier to recognize, occasionally blood vessels can mimic large myelinated axons and thus fiber misrecognition is not limited to small axons only. Quantification of inter-center recognition rates showed that the percentage of misrecognition ranged from 1.4% to 14.1% while the percentage of objects that raised doubts in the observer ranged from 5.9% to 9.1%. A mismatch between light microscopy- and electron microscopy-derived fiber counts was previously reported (Schmalbruch, 1986; Castro et al., 2008), but was not assessed by analysis of consecutive semi-thin and thin sections for particle recognition and apparently was due to mismatches between reference areas at the light and electron microscopic sections. Taken together, this clearly points to nerve fiber recognition as one of the key issues in peripheral nerve stereology especially when comparison of data obtained in different labs is sought.

To cope with this latter source of bias, we recommend that nerve fiber stereology be carried out by researchers experienced with this particular type of tissue. However, results of the present study showed that experience alone is not sufficient and thus we recommend that when a stereological study of peripheral nerve fibers is carried out for the first time by a research group, a calibration study should be performed to avoid errors in the practical application of the method (Geuna, 2000; Farel, 2002; von Bartheld, 2002). Naturally, tissue of adequate morphological quality is needed for meaningful quantitative analysis (Ward et al., 2008). A simple and effective verification method for quality control of morphoquantitative procedures has been proposed by von Bartheld (2002) and proved to be a valuable tool that can be adopted to ensure that the bias of the counting method adopted is reasonably “under control”. We designed a Nerve Fiber Recognition Test (based on the same test that we used in this study and that can be found as supplementary material of this article). This test can be completed by a researcher any time he/she starts carrying out stereological estimates (especially if it is the first time or if refresher training is needed). The test is based on three nerve micrographs (Supplementary Figs. 1–3) where a number of “objects” that resemble myelinated nerve fibers are indicated by a small open circle. The test-taker is asked to color-code green all circles corresponding to objects that he/she considers axons, to code red all circles corresponding to other tissue structures and finally to code yellow all those in doubt. In the second set of the same three micrographs (Supplementary Figs. 4–6), correct answers are given based on electron microscopic verification. The researcher can thus not only assess his/her recognition rate but also learn from the errors and be trained to reduce the number of errors in subsequent field work. This tool should assist in reducing inter-operator variability.

One potential solution for avoiding the problem of nerve fiber misrecognition is to carry out all fiber counts at the electron microscope level. However, this type of analysis, besides being far too laborious, would be in most cases not feasible since the entire nerve profile is too large to be included in a single thin section. This would make it impossible to sample fibers throughout the entire nerve, a basic requisite for stereology.

The difficulties in recognizing myelinated nerve profiles are also, in our opinion, an argument against the use of fully automated devices that have been developed for nerve fiber counting (Heijke et al., 2000; Lindemuth et al., 2002; Weyn et al., 2005; Hunter et al., 2007; Matiasek et al., 2008). In fact, although these devices are characterized by a high efficiency and make it possible to evaluate some additional spatial parameters of nerve fibers, such as their position within a nerve, their performance must remain under the careful "supervision" of the investigator in order to cope with the intrinsic rigidity of the machinery which can hardly adapt with the high variability in staining standards that makes the automatic recognition of nerve profiles problematic.

The choice of peripheral nerve slices for carrying out this methodological study has been motivated not only by the specific research interest of the authors, but also by the continuously increasing number of papers reporting quantitative data on peripheral nerve fibers, reflecting the increasing clinical importance of peripheral nerve injury and disease and their treatment (Vleggeert-Lankamp, 2007; Battiston et al., 2009; Dahlin et al., 2009; Siemionow and Brzezicki, 2009). Studies of this type may also be carried out in other fields (i.e. quantification of brain and renal morphology) and some of our findings likely are relevant to the quantification of spherical objects, although, to our knowledge, this is the first time that inter-procedure and inter-laboratory variability in stereology has been assessed.

In conclusion, results of the present study tell us that although great progress has been made in design-based stereological methods and sampling schemes, these procedures should not be considered a priori correct and superior to all other methods. It has been stated that there is no absolutely correct method for solving any problem that involves inductive reasoning (Smith, 1994; Geuna, 2005). The results of our study, as well as the lessons of many years of quantitative morphological assessment of biological structures, remind us that we should always be cautious when we handle quantitative data, even when the data were produced by design-based stereological methods.

References

- Acar M, Karacalar A, Ayyildiz M, Unal B, Canan S, Agar E, et al. The effect of autogenous vein grafts on nerve repair with size discrepancy in rats: an electrophysiological and stereological analysis. *Brain Res* 2008;1198:171–81.
- Baquet ZC, Williams D, Brody J, Smeyne RJ. A comparison of model-based (2D) and design-based (3D) stereological methods for estimating cell number in the substantia nigra pars compacta (SNpc) of the C57BL/6J mouse. *Neuroscience* 2009;161:1082–90.
- Baryshnikova LM, Von Bohlen Und Halbach O, Kaplan S, Von Bartheld CS. Two distinct events, section compression and loss of particles (“lost caps”), contribute to z-axis distortion and bias in optical disector counting. *Microsc Res Tech* 2006;69:738–56.
- Basgen JM, Nicholas SB, Mauer M, Rozen S, Nyengaard JR. Comparison of methods for counting cells in the mouse glomerulus. *Nephron Exp Nephrol* 2006;103:139–48.
- Battiston B, Raimondo S, Tos P, Gaidano V, Audisio C, Scevola A, et al. Tissue engineering of peripheral nerves. *Int Rev Neurobiol* 2009;87:227–49.
- Benes FM, Lange N. Two-dimensional versus three-dimensional cell counting: a practical perspective. *Trends Neurosci* 2001;24:11–7.
- Canan S, Bozkurt HH, Acar M, Vlamings R, Aktas A, Sahin B, et al. An efficient stereological sampling approach for quantitative assessment of nerve regeneration. *Neuropathol Appl Neurobiol* 2008a;34:638–49.
- Canan S, Aktas A, Ulkay B, Colakoglu S, Ragbetli MC, Ayyildiz M, et al. Prenatal exposure to a non-steroidal anti-inflammatory drug or saline solution impair sciatic nerve morphology: a stereological and histological study. *Int J Dev Neurosci* 2008b;26:733–8.
- Cassel CM, Särndal CE, Wretman JH. *Foundations of inference in sampling*. Malabar, FL: Krieger Publishing Company; 1993.
- Castro J, Negrodo P, Avendano C. Fiber composition of the rat sciatic nerve and its modification during regeneration through a sieve electrode. *Brain Res* 2008;1190:65–77.
- Clarke PG, Oppenheim RW. Neuron death in vertebrate development: in vitro methods. *Methods Cell Biol* 1995;46:277–321.
- Coggeshall RE, Lekan HA. Methods for determining numbers of cells and synapses: a case for more uniform standards of review. *J Comp Neurol* 1996;364:6–15.
- Dahlin L, Johansson F, Lindwall C, Kanje M. Future perspective in peripheral nerve reconstruction. *Int Rev Neurobiol* 2009;87:507–30.
- Di Scipio F, Raimondo S, Tos P, Geuna S. A simple protocol for paraffin-embedded myelin sheath staining with osmium tetroxide for light microscope observation. *Microsc Res Tech* 2008;71:497–502.
- Farel PB. Trust, but verify: the necessity of empirical verification in quantitative neurobiology. *Anat Rec* 2002;269:157–61.
- Gardella D, Hatton WJ, Rind HB, Rosen GD, von Bartheld CS. Differential tissue shrinkage and compression in the z-axis: implications for optical disector counting in vibratome, plastic and cryosections. *J Neurosci Methods* 2003;124:45–59.
- Geuna S. Appreciating the difference between design-based and model-based sampling strategies in quantitative morphology of the nervous system. *J Comp Neurol* 2000;427:333–9.
- Geuna S. The revolution of counting “tops”: two decades of the disector principle in morphological research. *Microsc Res Tech* 2005;66:270–4.
- Geuna S, Varejão AS. Evaluation methods in the assessment of peripheral nerve regeneration. *J Neurosurg* 2008;109:360–2.
- Geuna S, Borrione P, Corvetti G, Poncino A, Giacobini-Robecchi MG. Types and sub-types of neurons in dorsal root ganglia of the lizard *Podarcis sicula*: a light and electron microscope study. *Eur J Morphol* 1998;36:37–47.
- Geuna S, Tos P, Battiston B, Guglielmone R. Verification of the two-dimensional disector, a method for the unbiased estimation of density and number of myelinated nerve fibers in peripheral nerves. *Ann Anat* 2000;182:23–34.
- Guillery RW. On counting and counting errors. *J Comp Neurol* 2002;447:1–7. Guillery RW, August BK. Doubt and certainty in counting. *Prog Brain Res* 2002;135:25–42.

- Guillery RW, Herrup K. Quantification without pontification: choosing a method for counting objects in sectioned tissues. *J Comp Neurol* 1997;386:2–7.
- Gundersen HJG. Estimators of the number of objects per area unbiased by edge effects. *Microsc Acta* 1978;81:107–17.
- Gundersen HJ. Stereology of arbitrary particles. A review of unbiased number and size estimators and the presentation of some new ones, in memory of William R. Thompson. *J Microsc* 1986;143:3–45.
- Gundersen HJG, Jensen EB. The efficiency of systematic sampling in stereology and its prediction. *J Microsc* 1987;147:229–63.
- Gundersen HJ, Osterby R. Optimizing sampling efficiency of stereological studies in biology: or 'do more less well!'. *J Microsc* 1981;121:65–73.
- Gundersen HJG, Bendtsen TF, Korbo L, Marcussen N, Møller A, Nielsen K, et al. Some new, simple and efficient stereological methods and their use in pathological research. *APMIS* 1988a;96:379–94.
- Gundersen HJG, Bagger P, Bendtsen TF, Evans SM, Korbo L, Marcussen N, et al. The new stereological tools: disector, fractionator, nucleator and point sampled intercepts and their use in pathological research and diagnosis. *APMIS* 1988b;96:857–81.
- Gundersen HJG, Jensen EBV, Kieu K, Nielsen J. The efficiency of systematic sampling in stereology—reconsidered. *J Microsc* 1999;193:199–211.
- Hatton WJ, von Bartheld CS. Analysis of cell death in the trochlear nucleus of the chick embryo: calibration of the optical disector counting method reveals systematic bias. *J Comp Neurol* 1999;409:169–86.
- Heijke GC, Klopper PJ, Baljet B, Van Doorn IB, Dutrieux RP. Method for morphometric analysis of axons in experimental peripheral nerve reconstruction. *Microsurgery* 2000;20:225–32.
- Howard CV, Reed MG. Unbiased stereology. Three-dimensional measurement in microscopy. New York: Springer; 1998.
- Hunter DA, Moradzadeh A, Whitlock EL, Brenner MJ, Myckatyn TM, Wei CH, et al. Binary imaging analysis for comprehensive quantitative histomorphometry of peripheral nerve. *J Neurosci Methods* 2007;166:116–24.
- Hyman BT, Gomez-Isla T, Irizarry MC. Stereology: a practical primer for neuropathology. *J Neuropathol Exp Neurol* 1998;57:305–10.
- Kaplan S, Canan S, Aslan H, Unal B, Sahin B. A simple technique to measure the movements of the microscope stage along the x and y axes for stereological methods. *J Microsc (Oxford)* 2001;203:321–5.
- Kaplan S, Gökyar A, Ünal B, Turkkani-Tunc A, Bahadir A, Aslan H. A simple technique for localizing consecutive fields for disector pairs in light microscopy: application to neuron counting in rabbit spinal cord following spinal cord injury. *J Neurosci Methods* 2005;145:277–84.
- Larsen JO. Stereology of nerve cross sections. *J Neurosci Methods* 1998;85:107–18.
- Lindemuth R, Ernzerhof C, Schimrigk K. Comparative morphometry of myelinated nerve fibres in the normal and pathologically altered human sural and tibial nerve. *Clin Neuropathol* 2002;21:29–34.
- Matiasek K, Gais P, Rodenacker K, Jütting U, Tanck JJ, Schmahl W. Stereological characteristics of the equine accessory nerve. *Anat Histol Embryol* 2008;37: 205–13.
- Mayhew TM. An efficient sampling scheme for estimating fibre number from nerve cross sections: the fractionator. *J Anat* 1988;157:127–34.
- Mouton PR. Principles and practices of unbiased stereology. Baltimore: Johns Hopkins University Press; 2002.
- Popken GJ, Farel PB. Reliability and validity of the physical disector method for estimating neuron number. *J Neurobiol* 1996;31:166–74.
- Pover CM, Coggeshall RE. Verification of the disector method for counting neurons, with comments on the empirical method. *Anat Rec* 1991;231:573–8.
- Raimondo S, Fornaro M, Di Scipio F, Ronchi G, Giacobini-Robecchi MG, Geuna S. Methods and protocols in peripheral nerve regeneration experimental research. Part II. Morphological techniques.

- Int Rev Neurobiol 2009;87:79–101.
- Robinson G, Gray T. Electron microscopy. 2. Practical procedures. In: Bancroft JD, Stevens A, editors. Theory and practice of histological techniques. 4th ed. New York: Churchill Livingstone; 1996. p. 585–626.
- Schmalbruch H. Fiber composition of the rat sciatic nerve. *Anat Rec* 1986;215: 71–81.
- Schmitz C. Variation of fractionator estimates and its prediction. *Anat Embryol (Berl)* 1998;198:371–97.
- Schmitz C, Hof PR. Design-based stereology in neuroscience. *Neuroscience* 2005;130:813–31.
- Schmitz C, Korr H, Heinsen H. Design-based counting techniques: the real problems. *Trends Neurosci* 1999;22:345–6.
- Siemionow M, Brzezicki G. Current techniques and concepts in peripheral nerve repair. *Int Rev Neurobiol* 2009;87:141–72.
- Slomianka L, West MJ. Estimators of the precision of stereological estimates: an example based on the CA1 pyramidal cell layer of rats. *Neuroscience* 2005;136:757–67.
- Smith TMF. Sample surveys 1975–1990: an age of reconciliation? *Int Stat Rev* 1994;62:5–34.
- Sterio DC. The unbiased estimation of number and size of arbitrary particles using the disector. *J Microsc* 1984;134:127–36.
- Vleggeert-Lankamp CL. The role of evaluation methods in the assessment of peripheral nerve regeneration through synthetic conduits: a systematic review. *J Neurosurg* 2007;107:1168–89.
- von Bartheld CS. Comparison of 2-D and 3-D counting: the need for calibration and common sense. *Trends Neurosci* 2001;24:504–6.
- von Bartheld CS. Counting particles in tissue sections: choices of methods and importance of calibration to minimize bias. *Histol Histopathol* 2002;17: 639–48
- von Bartheld, C.S. Distribution of particles in the z-axis of tissue sections: relevance for counting methods. *NeuroQuantology*, in press.
- Ward TS, Rosen GD, von Bartheld CS. Optical disector counting in cryosections and vibratome sections underestimates particle numbers: effects of tissue quality. *Microsc Res Tech* 2008;71:60–8.
- West MJ. Stereological methods for estimating the total number of neurons and synapses: issues of precision and bias. *Trends Neurosci* 1999;22:51–61.
- Weyn B, van Remoortere M, Nuydens R, Meert T, van de Wouwer G. A multi-parametric assay for quantitative nerve regeneration evaluation. *J Microsc* 2005;219:95–101.